Eur. J. Mineral.
2012, **24**, 913–922
Published online March 2012

New nickel-uranium-arsenic mineral species from the oxidation zone of the Belorechenskoye deposit, Northern Caucasus, Russia: I. Rauchite, $Ni(UO_2)_2(AsO_4)_2 \cdot 10H_2O$, a member of the autunite group

IGOR V. PEKOV[1,*], VIKTOR V. LEVITSKIY[2], SERGEY V. KRIVOVICHEV[3], ANDREY A. ZOLOTAREV[3], IGOR A. BRYZGALOV[1], ALEKSANDR E. ZADOV[4] and NIKITA V. CHUKANOV[5]

[1] Faculty of Geology, Moscow State University, Vorobievy Gory, 119991 Moscow, Russia
*Corresponding author, e-mail: igorpekov@mail.ru
[2] Russian Minerals Co., 1st Krasnoselskiy per. 3, 107140 Moscow, Russia
[3] Faculty of Geology, St Petersburg State University, University Embankment 7/9, 199034 St Petersburg, Russia
[4] NPP ''Teplokhim'', Dmitrovskoye avenue 71, 127238 Moscow, Russia
[5] Institute of Problems of Chemical Physics, 142432 Chernogolovka, Moscow, Russia

Abstract: Rauchite, ideally $Ni(UO_2)_2(AsO_4)_2 \cdot 10H_2O$ (IMA no. 2010-037), a new arsenate mineral species of the autunite group, was found at the Belorechenskoye deposit, Adygea Republic, Northern Caucasus, Russia. It is a supergene mineral associated with dymkovite, annabergite and goethite in cavities of a dolomite vein with primary uraninite (pitchblende), nickeline and gersdorffite. Rauchite forms pseudo-tetragonal lamellar crystals (the main form is {001}) up to 0.5 mm across, typically split, like a fan or open book, and their clusters or crusts as large as 2 mm. Rauchite is transparent to translucent and light yellowish-green. The lustre is vitreous. The mineral is brittle, the Mohs' hardness is *ca.* 2. The cleavage is {001} perfect. D_{calc} is 3.427 g cm^{-3}. Rauchite is optically biaxial (−), $\alpha = 1.550(3)$, $\beta = 1.578(1)$, $\gamma = 1.581(1)$, $2V_{meas} = 40(5)°$, $2V_{calc} = 36°$. The average chemical composition (mean of eight electron-microprobe analyses) is (in wt%): MgO = 0.71, CoO = 0.07, NiO = 5.38, ZnO = 0.08, P_2O_5 = 1.08, As_2O_5 = 20.26, UO_3 = 54.22, H_2O_{calc} = 17.10, and the total = 98.90. The empirical formula calculated on the basis of 22 O *apfu* is: $(Ni_{0.76}Mg_{0.19}Co_{0.01}Zn_{0.01})_{\Sigma 0.97}U_{2.00}O_4$ $(As_{1.86}P_{0.16})_{\Sigma 2.02}O_8 \cdot 10H_2O$. Rauchite is triclinic, space group *I*-1, a = 7.100(3), b = 7.125(3), c = 19.955(8) Å, α = 92.406(14), β = 94.924(14), γ = 90.420(6)°, V = 1004.7(7) Å^3, Z = 2. [parameters of the reduced *P* cell are: a = 7.100(3), b = 7.125(3), c = 10.751(4) Å, α = 106.855(7), β = 104.366(7), γ = 90.420(6)°, V = 502.4(4) Å^3, Z = 1]. The crystal structure was refined from single-crystal X-ray diffraction data obtained at 153 K (R_1 = 0.089). The structure is based upon autunite-type $[(UO_2)[AsO_4]]^-$ layers with Ni^{2+} coordinated by six H_2O molecules and located in the interlayer space. The strongest lines in the powder X-ray diffraction pattern are [*d* in Å (*I*)(*hkl*)]: 9.97(100)(002), 6.641(22)(003), 4.936(62)(004, 01-3, −111), 4.533(41)(−112), 3.539(93)(020, 200, 20-1, 01-5, 02-1), 3.388(43)(20-2, 015, 02-2, 105), 2.488(27)(220, 2-21, −125, 1-25, 22-2, −222), and 2.233(27)(1-31, 3-10, 13-1, 31-1, 31-2, 2-24, 13-2, 21-7). The structure of rauchite corresponds to the 1*A*-type stacking arrangement of uranyl arsenate layers in the autunite group of minerals and synthetic compounds. The mineral is named in accordance with the naming rules accepted for the autunite group as the hydrated analogue of metarauchite, $Ni(UO_2)_2(AsO_4)_2 \cdot 8H_2O$.

Key-words: rauchite, new mineral species, arsenate, autunite group, uranium mica, crystal structure, oxidation zone, Belorechenskoye deposit, Adygea, Russia.

1. Introduction

The Belorechenskoye deposit is located in the upper reaches of the small river Syuk, a tributary of the Belaya river, 60 km to the south of the city of Maikop, Adygea Republic, Northern Caucasus, Russia. It is a complex deposit consisting of two systems of different hydrothermal veins cross-cutting Paleozoic gneisses, amphibolites, and granite-gneisses, and the granites and serpentinized ultrabasites of the Dakhovskaya intrusion. The earlier dolomite veins containing rich U and Ni mineralization (mainly pitchblende and Ni arsenides) were actively prospected for U, with underground workings, in 1960s. In this period, the deposit was known as the Dakhovskoye U deposit. The younger barite and calcite-barite veins were prospected for barite in the 1970s, and the deposit was named Belorechenskoye. The original geological data on the deposit were published by Dymkov *et al.* (1970) and Semashko & Pakul'nis (1971). The mineralogical composition and the formation of the different veins of the deposit were studied by Dymkov *et al.* (1970), Melkov & Sergeeva (1971), Zubov & Kazantsev (1970), Krivovichev (1972,

0935-1221/12/0024-2217 $ 4.50
DOI: 10.1127/0935-1221/2012/0024-2217

1973, 1975), Granovskaya (1984), Pekov (1993), and Pekov *et al*. (2010). The latter paper summarizes the earlier published information on the history and on the geological and mineralogical features of the Belorechenskoye deposit.

The oxidation zone is poorly developed at Belorechenskoye. The oxidized ores occur in several areas, mainly in upper part of the deposit. The supergene mineralization was systematically studied only recently, in 1990s–2000s, by the authors (I.V.P & V.V.L.). In the oxidized parts of the dolomite veins with Ni arsenides (nickeline, krutovite, rammelsbergite) and gersdorffite, or with native As, secondary minerals include goethite (limonite) and a number of arsenates: annabergite, pharmacolite, picropharmacolite, hörnesite, rösslerite, parasymplesite, and nováčekite; gypsum, aragonite, arsenolite, schröckingerite and rabbittite have also been found here. In the oxidation zone of the barite and calcite-barite veins with galena, sphalerite, chalcopyrite, pyrite and marcasite, the supergene minerals include abundant limonite, various sulfates (jarosite, gypsum, melanterite, brochantite, antlerite, devilline, serpierite, anglesite) and carbonates (malachite, azurite, cerussite); coronadite, hemimorphite, and native sulfur have also been observed (Pekov *et al*., 2010).

In 2010, one of the authors (V.V.L.) found in Adit #1, the hypsometrically uppermost underground working at the deposit, a new small occurrence of secondary minerals related to a dolomite vein with rich Ni and U mineralization. In this supergene assemblage, two new hydrous Ni-U-As-O mineral species were discovered: the arsenite dymkovite, $Ni(UO_2)_2(As^{3+}O_3)_2 \cdot 7H_2O$ (IMA no. 2010-087; Pekov *et al*., 2012), and a new member of the autunite group, *rauchite*, $Ni(UO_2)_2(As^{5+}O_4)_2 \cdot 10H_2O$, described herein.

Rauchite is named in accordance with the naming rules accepted for the autunite group, as the hydrated analogue of metarauchite, $Ni(UO_2)_2(AsO_4)_2 \cdot 8H_2O$, a mineral recently described by Plášil *et al*. (2010). The root name was given by Plášil *et al*. (2010) in memory of the Czech mineral collector Luděk Rauch (1951–1983) who died in the Jáchymov mines, Czech Republic, during a prospecting trip. Both the mineral data and the name have been approved by the IMA Commission on New Minerals, Nomenclature and Classification (IMA no. 2010-037).

The type specimen of rauchite is deposited in the Fersman Mineralogical Museum of the Russian Academy of Sciences, Moscow, Russia, registration number 3997/1.

2. Occurrence and general appearance

Rauchite was found in small cavities and cracks of a slightly oxidized dolomite vein containing abundant nests of intimately intergrown uraninite (pitchblende), nickeline and gersdorffite. Pitchblende and nickeline together form concentric kidney-shaped or dendritic aggregates up to 2–3 cm embedded in pinkish, greenish or pale cream-coloured veiny dolomite. Gersdorffite overgrows nickeline forming rims (up to 1 mm thick) or crusts of cubic or cubo-octahedral crystals (up to 0.5 mm across). Minor amounts of other primary minerals were observed, mainly within cavities: sphalerite, pyrite, millerite, dickite, calcite, and quartz.

Rauchite is closely associated with nickeline, gersdorffite, and pitchblende, which were obviously a primary source of U, Ni and As for its formation. Other supergene minerals associated with rauchite are dymkovite, annabergite, and goethite (limonite).

Rauchite looks like other U micas. It occurs as pseudotetragonal (quadratic or, more often, rectangular) lamellar crystals up to 0.5 mm in size. The major form is the {001} pinacoid, the lateral faces are very narrow and could not be indexed. Rauchite crystals are typically split, forming aggregates resembling a propeller or open book, and occur as clusters or crusts up to 2 mm across on the surface of dolomite or as overgrowth on aggregates of pitchblende, nickeline, and gersdorffite (Fig. 1). Near-parallel or chaotic aggregates of rauchite lamellae fill small cracks in the pitchblende-nickeline nests forming veinlets that are $\leq$0.5 mm thick and $\leq$3 mm long.

3. Physical properties and optical characteristics

Rauchite is transparent to translucent, light yellowish-green, the smallest crystals being pale green. The streak is white. The lustre is vitreous or, on the {001} cleavage surfaces, pearly. Rauchite is non-fluorescent in both ultraviolet and cathode rays. It is brittle, the Mohs' hardness is *ca.* 2. The cleavage is perfect on {001}, micaceous, the fracture is laminated. Our attempts to measure density gave unsatisfactory result because of the open-work character of rauchite aggregates. The calculated density is 3.427 g cm^{-3}. The mineral is radioactive.

Rauchite is optically biaxial (−), $\alpha = 1.550(3)$, $\beta = 1.578(1)$, $\gamma = 1.581(1)$, $2V_{meas} = 40(5)°$, $2V_{calc} = 36°$. Dispersion was not observed. Orientation: X is approximately perpendicular to (001), Y and Z are close to the diagonals of square-shape crystals in the (001) plane. Under the microscope, rauchite is colourless.

4. IR spectroscopy

Rauchite powder was mixed with anhydrous KBr, pelletized, and analyzed using a Bruker Alpha spectrophotometer. Polystyrene and gaseous NH_3 were used as frequency standards; the precision of frequency measurement is ± 1 cm^{-1}; the mean resolution for the range 400–1600 cm^{-1} is 0.8 cm^{-1}.

The IR spectrum of rauchite (Fig. 2) is similar to those of other autunite group minerals. Absorption bands in the IR spectrum of rauchite and their assignments (cm^{-1}; s – strong band, sh – shoulder) are: 3440s, 3370s (O-H-stretching vibrations of H_2O molecules), 1650 (H-O-H bending vibrations of H_2O molecules), 1035 (P-O stretching

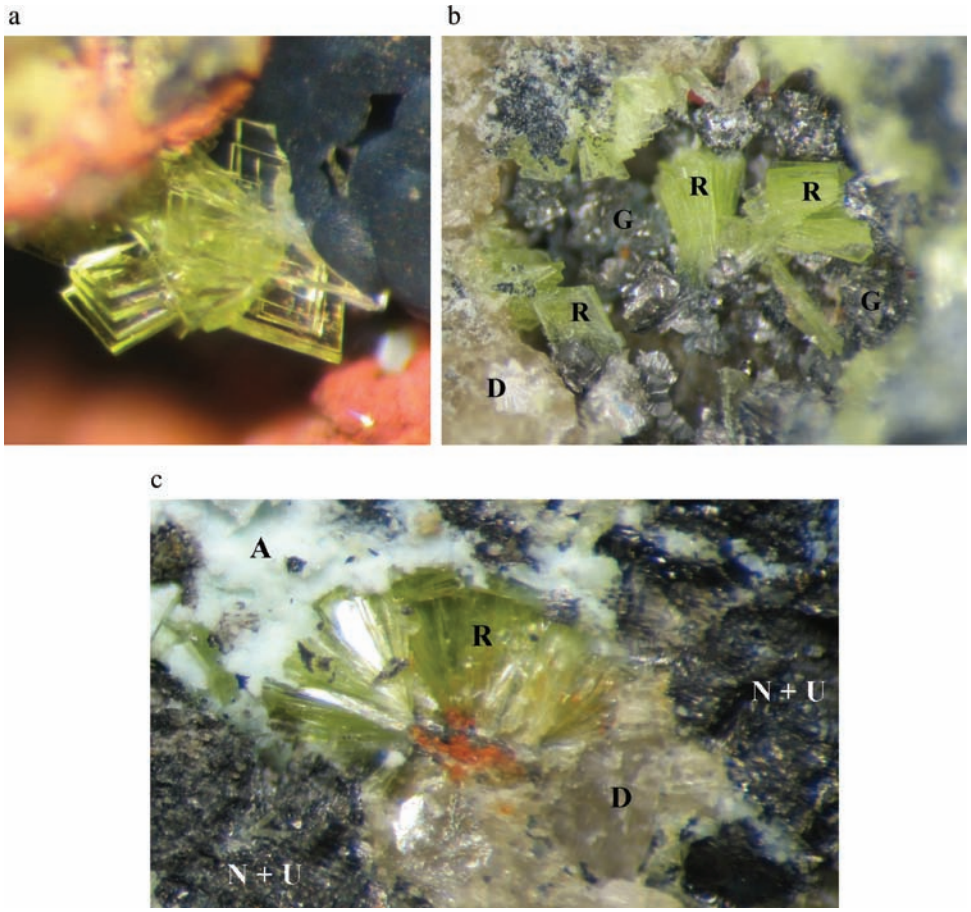

Fig. 1. Crystals and aggregates of rauchite. (a) cluster of rauchite crystals on goethite in cavity. Image width = 0.9 mm. (b) split crystals of rauchite on gersdorffite crystalline crust incrusting a cavity in dolomite. Image width = 2.1 mm. (c) propeller-shaped aggregate of rauchite on dolomite with nickeline-uraninite nests and the youngest supergene annabergite. Image width = 1.8 mm.
Abbreviations: A – annabergite, D – dolomite, G – gersdorffite, N – nickeline, R – rauchite, U – uraninite (pitchblende). Photos by I.V. Pekov and A.V. Kasatkin.

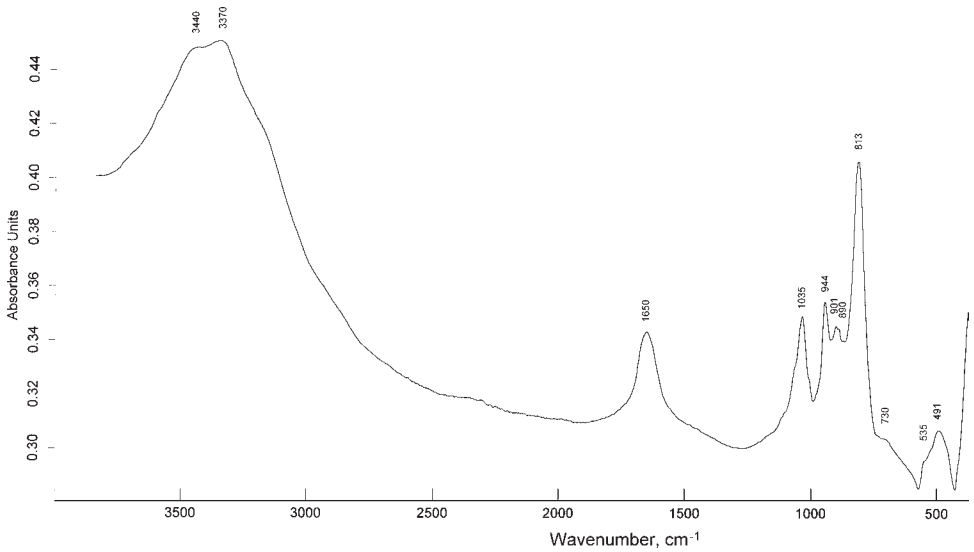

Fig. 2. IR spectrum of rauchite.

vibrations of admixed PO_4^{3-} anions), 944, 901, 890 (asymmetric U-O stretching vibrations of UO_2^{2+} cations), 813s (As-O stretching vibrations of AO_4^{3-} anions), 730sh (unassigned), 535sh (O-P-O bending vibrations of PO_4^{3-} anions), 491 (libration mode of H_2O molecules). Unlike metarauchite showing a singlet in the range of 3300–3500 cm^{-1} (Plášil *et al*., 2010), rauchite shows two absorption maxima in this region and additional splitting of the band of U-O stretching vibrations near 900 cm^{-1}.

5. Chemical data

The chemical composition of rauchite was determined by electron microprobe (in wavelength-dispersive mode) with a Camebax SX 50 instrument, operating at a voltage of 15 kV and a beam current of 30 nA. The electron beam was rastered on an area of 10×10 μm^2 to minimize damage to the highly hydrated mineral. The following standards were used: olivine (Mg), Co (Co), NiO (Ni), ZnO (Zn), $KTiPO_5$ (P), tilasite (As), and UO_2 (U). Contents of Na, K, Ca, Sr, Ba, Pb, Mn, Fe, Cu, Al, V, Si, S, F, and Cl are generally below detection limits; in some points CaO, FeO, or CuO contents are up to 0.05–0.07 wt%.

H_2O was not measured because of scarcity of pure material, but its presence was confirmed by IR spectroscopy (see above). Content of H_2O was determined from structural data (see below), and are in good agreement with the deficiency seen in the analytical total.

The average (eight analyses) chemical composition of rauchite (in wt%, ranges are given in parentheses) is: MgO = 0.71 (0.3–1.2), CoO = 0.07 (0.00–0.15), NiO = 5.38 (5.0–6.1), ZnO = 0.08 (0.00–0.2), P_2O_5 = 1.08 (0.8–1.2), As_2O_5 = 20.26 (19.4–20.8), UO_3 = 54.22 (53.4–55.1), H_2O_{calc} = 17.10, and total = 98.90. The H_2O content was calculated for 10 molecules *pfu*, according to the structural data.

The empirical formula of rauchite, calculated on the basis of 22 O *apfu*, is $(Ni_{0.76}Mg_{0.19}Co_{0.01}Zn_{0.01})_{\Sigma 0.97}U_{2.00}O_4(As_{1.86}P_{0.16})_{\Sigma 2.02}O_8 \cdot 10H_2O$.

The simplified, end-member formula is $Ni(UO_2)_2(AsO_4)_2 \cdot 10H_2O$, corresponding to (in wt%): NiO 7.07, As_2O_5 21.75, UO_3 54.13, H_2O 17.05, and a total of 100.00.

6. X-ray crystallography

Single-crystal X-ray studies of rauchite were carried out using a Bruker SMART APEX CCD diffractometer at 153 K in order to prevent possible dehydration of the mineral. A primitive triclinic unit cell was determined with the unit-cell parameters: $a = 7.100(3)$, $b = 7.125(3)$, $c = 10.751(4)$ Å, $\alpha = 106.855(7)$, $\beta = 104.366(7)$, $\gamma = 90.420(6)°$, $V = 502.4(4)$ Å^3, $Z = 1$. The a:b:c ratio is 0.997:1:1.509. In order to compare rauchite with other decahydrates of the autunite group with medium-size octahedral divalent cations, this cell was transformed into an *I*-centered unit cell using the transformation matrix [−100 / 0−10 / 112], which provided the following unit-cell parameter s: $a = 7.100(3)$, $b = 7.125(3)$, $c = 19.955(8)$ Å, $\alpha = 92.406(14)$, $\beta = 94.924(14)$, $\gamma = 90.420(6)°$, $V = 1004.7(7)$ Å^3, $Z = 2$. The a:b:c ratio is 0.997:1:2.801.

X-ray powder diffraction data of rauchite were collected using a STOE IPDS II diffractometer equipped with an image-plate detector, using the Gandolfi method (Mo$K\alpha$-radiation; detector-to-sample distance: 200 mm). Data are given in Table 1 (for d_{calc}, only reflections with intensities ≥ 1 are included). Triclinic unit-cell parameters refined using least-squares techniques from the powder data are: $a = 7.11(5)$, $b = 7.12(5)$, $c = 19.98(14)$ Å, $\alpha = 92.2(1)$, $\beta = 94.9(2)$, $\gamma = 90.2(1)°$, $V = 1007(4)$ Å^3.

Rauchite, like the majority of other highly hydrated U micas, is unstable under heating. It easily loses two H_2O molecules and transforms into metarauchite, $Ni(UO_2)_2(AsO_4)_2 \cdot 8H_2O$. The sample of rauchite heated to 40°C for 30 min produced an X-ray powder diffraction pattern with essentially weaker rauchite reflections, new strong reflections with d = 8.62, 5.99, 3.972 Å, and some other weak reflections corresponding to metarauchite (Plášil *et al*., 2010).

The extent of thermal expansion of rauchite is insignificant. The unit-cell volumes calculated from X-ray single-crystal data obtained at 153 K [502.4(4) Å^3] and from powder data at room temperature [500(3) Å^3] are the same within experimental error.

7. Crystal structure

The unit-cell parameters (see above) were refined using least-squares technique. The structure was solved and refined in the space group *I*-1 using the SHELX program package (Sheldrick, 2008). A twinning model was incorporated into the refinement using the matrix [100/010/00-1] (twinning along the (001) plane), which slightly improved the refinement and provided the ratio between the twin components 0.95:0.05. The low quality of the rauchite crystals was responsible for the rather large value of the crystallographic agreement R_1 index (0.089). Attempts to refine O atoms anisotropically were unsuccessful (most of the atoms appear to be non-positive definite) as were the attempts to determine the H sites. A series of relatively high peaks (6–15.4 $e \cdot$Å^{-3}) were observed in certain positions within the atomic plane occupied by heavy U and As atoms, which we interpret as resulting from stacking faults in the sequence of the uranyl arsenate layers (see below). The crystallographic and experimental parameters are given in Table 2, atom coordinates and displacement parameters in Table 3, and selected interatomic distances in Table 4.

The structure of rauchite (Fig. 3a) contains one symmetrically independent U^{6+} cation forming two short U=O bonds (1.75–1.77 Å) that define the uranyl cation and four longer U–O bonds (2.25–2.30 Å). The resulting UO_6 square bipyramids are linked via (As, P)O_4 tetrahedra to form autunite-type $[(UO_2)[(As,P)O_4]]^-$ layers coplanar to

Table 1. X-ray powder diffraction data of rauchite.

I_{obs}	d_{obs}	I_{calc}	d_{calc}	$h\ k\ l$
100	9.97	100	9.932	002
22	6.641	83	6.621	003
62	4.936	27, 26, 18	4.966, 4.955, 4.927	004, 01-3, −111
41	4.533	10	4.556	−112
5	4.302	8	4.305	112
93	3.539	30, 33, 21, 5, 21	3.559, 3.537, 3.535, 3.534, 3.530	020, 200, 20-1, 01-5, 02-1
43	3.388	12, 5, 11, 15	3.426, 3.407, 3.397, 3.343	20-2, 015, 02-2, 105
15	3.155	4, 5	3.153, 3.153	−121, 1-21
14	2.987	9, 6, 8, 7	3.006, 2.959, 2.954, 2.953	20-4, 21-3, 016, 0-24
15	2.879	6, 2, 4	2.904, 2.876, 2.836	106, 1-23, 024
3	2.755	4, 3, 2	2.770, 2.762, 2.747	204, 20-5, 213
4	2.667	4	2.675	01-7
27	2.488	7, 5, 3, 3, 5, 5	2.495, 2.493, 2.490, 2.488, 2.474, 2.463	220, 2-21, −125, 1-25, 22-2, −222
3	2.364	3, 2	2.369, 2.364	222, −216
27	2.233	3, 2, 2, 2, 2, 4, 2, 2, 4	2.246, 2.246, 2.245, 2.241, 2.239, 2.222, 2.221, 2.220, 2.218	1-31, 3-10, 13-1, 31-1, 31-2, 2-24, 13-2, 21-7
18	2.126	4, 2, 2, 2, 5, 3	2.146, 2.134, 2.122, 2.121, 2.109, 2.107	118, 312, −127, 1-27, 30-5, 034
5	2.044	3	2.046	−119
1	1.989	3	1.986	0.0.10
5	1.921	1, 1	1.924, 1.920	23-3, 3-22
3	1.897	2, 2, 2, 2	1.906, 1.904, 1.891, 1.891	1.1.-10, −233, 2-33, 036
2	1.858	2	1.860	03-7
6	1.828	2, 2	1.829, 1.825	1.-1.10, 32-5
15	1.769	4, 2, 3, 2	1.768, 1.767, 1.766, 1.765	400, 40-2, 041, 04-2
2	1.733	2, 2	1.736, 1.734	3-25, -326
9	1.677	1, 1	1.681, 1.680	1-38, 23-7
16	1.581	2, 2, 1, 2, 1, 1	1.587, 1.586, 1.585, 1.583, 1.582, 1.577	1.-1.12, 318, −422, 240, 24-2, 420
7	1.544	1, 1, 1	1.543, 1.541, 1.540	24-4, −3.1.10, 1.3.-10
2	1.488	1, 1	1.501, 1.481	1.-3.10, −1.3.10
5	1.397	1	1.394	3.1.-12

Table 2. Crystallographic data and refinement parameters for rauchite.

Crystal data	
Temperature	153 K
Radiation, wavelength	Mo$K\alpha$, 0.71073 Å
Crystal system	triclinic
Space group	I-1
Unit-cell dimensions a, b, c (Å), α, β, γ (°)	7.100(3), 7.125(3), 19.955(8), 92.406(14), 94.924(14), 90.420(60)
Unit-cell volume (Å^3)	1004.7(7)
Z	2
Calculated density (g/cm^3)	3.427
Absorption coefficient (mm^{-1})	19.765
Crystal size (mm^3)	0.07 × 0.07 × 0.01
Data collection	
θ range	2.05 − 28.00°
h, k, l ranges	−9→ 9, −9→ 8, −26→ 26
Total reflections collected	5410
Unique reflections (R_{int})	2402 (0.059)
Unique reflections $F > 4\sigma(F)$	2075
Structure refinement	
Refinement method	Full-matrix least-squares on F^2
Weighting coefficients a, b	0.1291, 193.5164
Extinction coefficient	0
Data/restraints/parameters	2402/0/73
R_1 [$F > 4\sigma(F)$], wR_2 [$F > 4\sigma(F)$],	0.089, 0.233
R_1 all, wR_2 all	0.100, 0.2410
Goodness-of-fit on F^2	1.119
Largest diff. peak and hole, e Å^{-3}	15.145, −3.923

Table 3. Coordinates, site-occupancies and displacement parameters (Å^2) of atoms in the structure of rauchite.

Atom	Occupancy	x	y	z	U_{iso}
U	U	0.76232 (11)	0.75189 (12)	0.54532 (4)	0.0133 (3)
As	$As_{0.89\ (2)}P_{0.11\ (2)}$	0.7494 (3)	0.2478 (3)	0.50112 (13)	0.0122 (8)
Ni	$Ni_{0.69\ (5)}Mg_{0.31\ (5)}$	1/4	−1/4	1/4	0.028 (2)
O1	O	0.717 (3)	0.072 (3)	0.5501 (9)	0.020 (4)
O2	O	0.737 (2)	0.734 (2)	0.4575 (8)	0.017 (3)
O3	O	0.808 (2)	0.432 (2)	0.5530 (8)	0.017 (3)
O4	O	0.785 (2)	0.764 (2)	0.6337 (8)	0.012 (3)
O5	O	0.550 (3)	0.293 (3)	0.4507 (9)	0.022 (4)
O6	O	0.080 (2)	0.801 (2)	0.5490 (8)	0.018 (3)
H_2O1	O	0.337 (4)	−0.522 (4)	0.2555 (13)	0.045 (6)
H_2O2	O	0.461 (4)	−0.186 (4)	0.1830 (12)	0.043 (6)
H_2O3	O	0.059 (4)	−0.318 (4)	0.1700 (13)	0.048 (6)
H_2O4	O	0.794 (4)	−0.010 (4)	0.3301 (13)	0.048 (6)
H_2O5	O	−0.179 (7)	0.087 (7)	0.175 (2)	0.094 (13)

Atom	U_{11}	U_{22}	U_{33}	U_{23}	U_{13}	U_{12}
U	0.0025 (4)	0.0080 (4)	0.0294 (5)	0.0027 (3)	0.0006 (3)	0.0011 (2)
As	0.0029 (12)	0.0076 (13)	0.0266 (15)	0.0036 (9)	0.0016 (8)	0.0015 (7)
Ni	0.034 (4)	0.033 (4)	0.018 (3)	−0.002 (2)	0.003 (2)	0.007 (3)

(001) (Fig. 3b). Divalent cations (Ni, Mg)$^{2+}$ are octahedrally coordinated by six H_2O molecules. The resulting [(Ni, Mg)$(H_2O)_6$]$^{2+}$ octahedra are located in the interlayer space and, along with two additional H_2O molecules provide linkage of adjacent layers via a system of H bonds (shown in Fig. 3a as dotted lines; the respective O···O distances are given in Table 4). Figure 3c shows a nodal representation (black-and-white graph) of the uranyl

Table 4. Selected interatomic distances (Å) in the structure of rauchite.

U-O2	1.745 (16)	O1···H_2O3	2.81 (3)
U-O4	1.755 (15)	O3···H_2O2	2.89 (3)
U-O5	2.246 (19)	O4···H_2O1	2.81 (3)
U-O6	2.275 (18)	O5···H_2O5	2.91 (5)
U-O1	2.304 (19)	O6···H_2O4	2.85 (3)
U-O3	2.315 (18)	H_2O1···H_2O5	2.74 (6)
		H_2O1···H_2O3	2.84 (4)
As-O1	1.648 (18)	H_2O1···H_2O2	2.92 (4)
As-O3	1.663 (17)	H_2O1···H_2O3	2.93 (4)
As-O6	1.665 (17)	H_2O2···H_2O4	2.81 (4)
As-O5	1.706 (19)	H_2O2···H_2O3	2.95 (4)
		H_2O2···H_2O3	2.98 (4)
Ni-H_2O1	2.04 (3) 2×	H_2O3···H_2O4	2.78 (4)
Ni-H_2O3	2.04 (3) 2×		
Ni-H_2O2	2.15 (3) 2×		

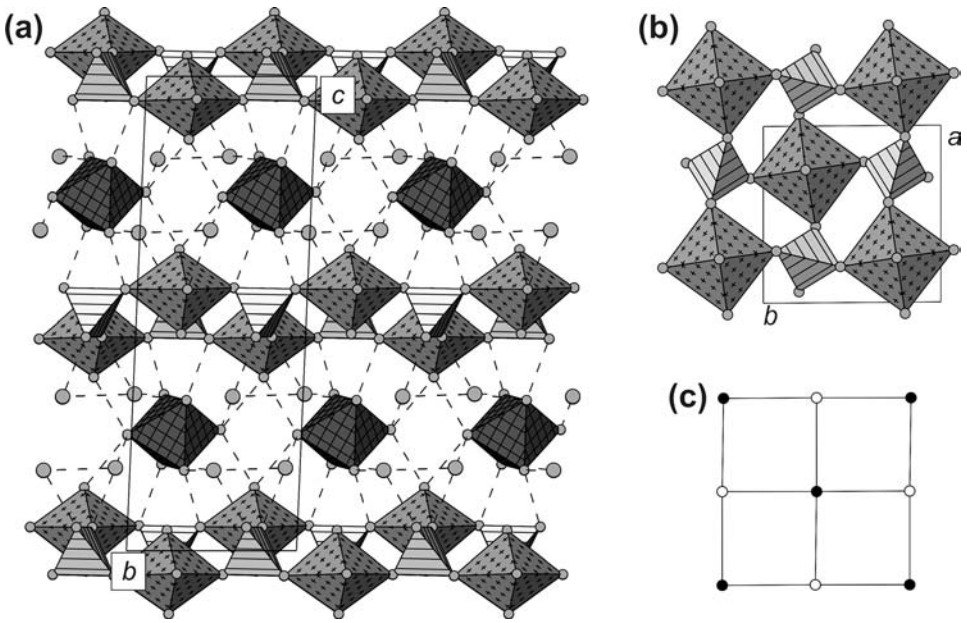

Fig. 3. The structure of rauchite. (a) projection along the *a*-axis, (b) top view of the uranyl arsenate layer, and (c) nodal representation. Notes: U polyhedra = cross-hatched, AsO_4 tetrahedra = lined, Ni polyhedra = checkered, H_2O molecules are shown as medium-sized circles, dotted lines indicate O···O contacts responsible for hydrogen bonds.

arsenate layer in the structure of rauchite (black and white nodes correspond to the U and As coordination centers, edges symbolize linkage of adjacent polyhedra *via* bridging O atoms).

8. Discussion

Rauchite is a new member of the autunite group of uranyl phosphates and arsenates (Locock, 2007a and b). From a chemical viewpoint, it is a high-hydrate analogue of metarauchite, $Ni(UO_2)_2(AsO_4)_2 \cdot 8H_2O$ (Plášil *et al*., 2010) and a low-hydrate analogue of $Ni(UO_2)_2(AsO_4)_2 \cdot 12H_2O$ known as synthetic compound (Chernorukov *et al*., 1998; Locock *et al*., 2004) (Table 5). A synthetic analogue of rauchite, $Ni(UO_2)_2(AsO_4)_2 \cdot 10H_2O$, was prepared by Chernorukov *et al*. (1998). Its X-ray powder pattern (JCPDS ICDD 52-0239) is similar to that of rauchite but no *hkl* indices, unit-cell dimensions or crystal system were reported. It is very likely that rauchite is the product of dehydration of the natural phase $Ni(UO_2)_2(AsO_4)_2 \cdot 12H_2O$, which has not been found as a mineral so far. Some evidence for this conclusion might be derived from the observed low quality of the rauchite crystals. A similar situation was reported by

Table 5. Comparative data for synthetic Ni $(UO_2)_2$ $(AsO_4)_2 \cdot 12H_2O$, rauchite and metarauchite.

Mineral/Compound Formula	Synthetic $Ni(UO_2)_2(AsO_4)_2 \cdot 12H_2O$	Rauchite $Ni(UO_2)_2(AsO_4)_2 \cdot 10H_2O$	Metarauchite $Ni(UO_2)_2(AsO_4)_2 \cdot 8H_2O$
Crystal system	Triclinic	Triclinic	Triclinic
Space group	$P\bar{1}$	$I\bar{1}$	$P\bar{1}$
Unit cell data			
a, Å	7.152	7.100	7.194
b, Å	7.158	7.125	9.713
c, Å	11.256	19.955	13.201
α, °	81.55	92.41	75.79
β, °	81.36	94.92	83.92
γ, °	88.92	90.42	81.59
V, Å^3	564	1005	882
Z	1	2	2
D(calc), g cm^{-3}	3.22	3.43	3.81
Optical data			
α	n.d.	1.550	1.625
β	n.d.	1.578	1.649
γ	n.d.	1.581	1.649
Optical sign, $2V_{meas}$	n.d.	(−) 40°	(−) 2V not measured
Reference	Locock *et al*. (2004)	this work	Plášil *et al*. (2010)

Locock *et al*. (2004), who prepared $Mg(UO_2)_2$ $(AsO_4)_2 \cdot 10H_2O$ (synthetic analogue of nováčekite II) by dehydration of crystals of the primary phase $Mg(UO_2)_2(AsO_4)_2 \cdot 12H_2O$ (synthetic analogue of nováčekite I). As in the case with rauchite, the structure model was obtained, but with rather high agreement index R_1 of 0.085. Locock *et al*. (2004) explained the low quality of the structure refinement by the high mosaicity of the crystals induced by dehydration and possible ongoing heat-load from the primary X-ray beam. Additional evidence may be deduced from the analysis of electron-density peaks observed in the difference Fourier map (Fig. 4). The highest peaks are located at the positions within the uranyl arsenate layers and may be viewed as resulting from stacking faults in the packing of the layers. In particular, one of the series of peaks correspond to the imaginary positions of the U and As atoms (depicted as *qU* and *qAs* in Fig. 4) if the layers are shifted along the *a* axis by 3.56 Å. Such stacking faults may well be associated with dehydration of the original dodecahydrate phase and subsequent rearrangement of the layer stacking.

The crystal chemistry of synthetic analogues of octa-, deca-, and dodecahydrate members of the autunite group and their synthetic analogues containing divalent transition metals and Mg was studied in details by Locock *et al*. (2004), who provided refined structure models for $Mg(UO_2)_2(AsO_4)_2 \cdot 10H_2O$ (synthetic analogue of nováčekite II), $Mn(UO_2)_2(PO_4)_2 \cdot 10H_2O$, $Co(UO_2)_2(PO_4)_2 \cdot 10H_2O$, and $Ni(UO_2)_2(PO_4)_2 \cdot 10H_2O$. The structure of another member of the group, saléeite, $Mg(UO_2)_2(PO_4)_2 \cdot 10H_2O$, was

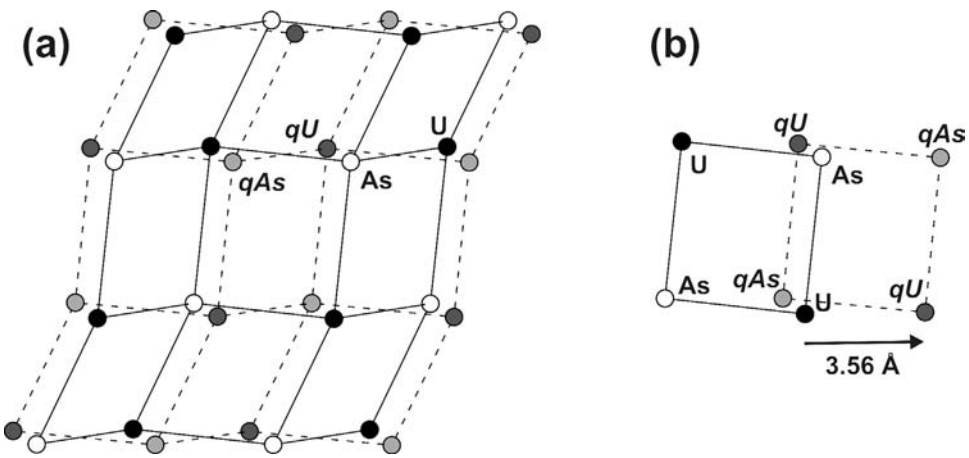

Fig. 4. Black-and-white graph of the uranyl arsenate layer in the structure of rauchite (*cf*. Fig. 3c) showing positions of the U and As atoms compared to the positions of the highest peaks in the Fourier difference electron density map (dark- and light-grey circles, respectively) (a). The appearance of the dummy peaks (*qU* and *qAs*) may be explained as being due to the stacking faults associated with the shift of the adjacent layers by 3.56 Å along the *a*-axis (b).

investigated by Miller & Taylor (1986). Crystallographic information on these phases is given in Table 6 (the unit-cell dimensions of rauchite are given in a body-centered triclinic cell setting). It should be noted that no polytypes are known in the autunite group to date, since all known chemical compositions crystallize in one unit cell each. Detailed analysis of the structures listed in Table 6 allowed for classification into three different groups according to the stacking arrangement of the uranyl arsenate/phosphate layers: (i) space group $P2_1/n$, (ii) space group $I2/m$, and (iii) space group $I\bar{1}$. Figure 5 provides comparison of the relative positions of the layers in three representative structures: $Mg(UO_2)_2(AsO_4)_2 \cdot 10H_2O$ (synthetic analogue of nováčekite II; Fig. 5a and d), $Mn(UO_2)_2(PO_4)_2 \cdot 10H_2O$ (Fig. 5b and e), and rauchite, $Ni(UO_2)_2(AsO_4)_2 \cdot 10H_2O$ (Fig. 5c and f). In order to simplify the procedure, the uranyl/phosphate layers are depicted as black-and-white graphs (Fig. 3c). In the structure of group (i), adjacent layers are displaced relative to each other in the horizontal plane by the vector **t** approximately parallel to **a**' + 3**b**', where **a**' and **b**' are two perpendicular vectors lying within the layer. The length of the displacement vector **t** is *ca*. 0.90 Å. In group (i), the sequence of displacement vectors along the stacking of the layers is. . .+**t, –t, +t, –t. . .**, and the primitive monoclinic unit

Table 6. Classification of minerals and synthetic compounds of the autunite group according to the stacking arrangement of the uranyl phosphate/arsenate layers.

Formula/mineral name	Sp. gr.	*a*, Å	*b*, Å	*c*, Å	α (°)	β (°)	γ (°)	Reference
2*M*-type stacking arrangement								
$Mg(UO_2)_2(AsO_4)_2 \cdot 10H_2O$ nováčekite II (synthetic)	$P2_1/n$	7.133	20.085	7.157	90	90.59	90	Locock *et al*. (2004)
$Mg(UO_2)_2(PO_4)_2 \cdot 10H_2O$ saléeite[a]	$P2_1/n$	6.951	19.947	6.977	90	90.55	90	Miller & Taylor (1986)
$Co(UO_2)_2(PO_4)_2 \cdot 10H_2O$	$P2_1/n$	6.949	19.935	6.962	90	90.44	90	Locock *et al*. (2004)
$Ni(UO_2)_2(PO_4)_2 \cdot 10H_2O$	$P2_1/n$	6.951	19.822	6.971	90	90.42	90	Locock *et al*. (2004)
1*M*-type stacking arrangement								
$Mn(UO_2)_2(PO_4)_2 \cdot 10H_2O$	$I2/m$	6.966	20.377	6.978	90	91.02	90	Locock *et al*. (2004)
1*A*-type stacking arrangement								
$Ni(UO_2)_2(AsO_4)_2 \cdot 10H_2O$ rauchite	$I\bar{1}$	7.100	7.125	19.955	92.41	94.92	90.42	this work

[a]Unit-cell dimensions transformed from the original setting reported by Miller & Taylor (1986) by applying matrix [100/010/101] as described by Locock *et al*. (2004).

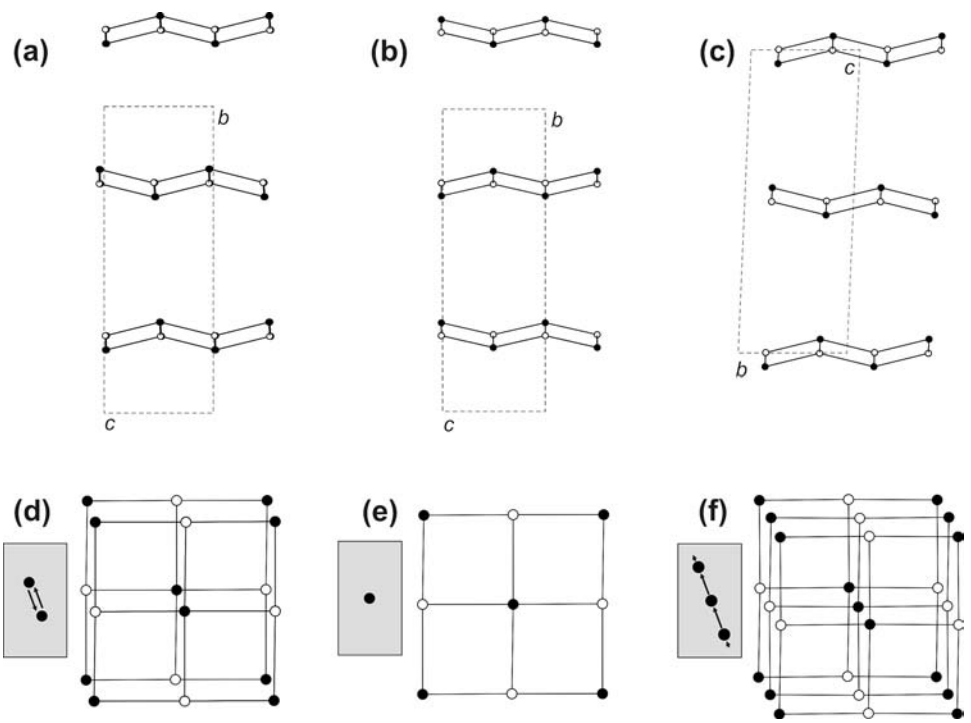

Fig. 5. Relative positions of uranyl phosphate/arsenate layers in three groups of natural and synthetic uranyl phosphate/arsenates of the autunite group: (a and d) 2*M*-stacking type, (b and e) 1*M*-stacking type, (c and f) 1*A*-stacking type. See text for details.

cell contains two translationally independent layers. In the structures of group (ii), there is no displacement of adjacent layers within the horizontal plane (**t** = 0), and the primitive monoclinic unit cell contains one layer. The structure of group (iii) (rauchite) is characterized by the sequence. . .+**t**, +**t**, +**t**, +**t**. . . and a primitive triclinic unit cell. Thus, the layer stacking in the three groups corresponds to the stacking of layers in the 2*M*, 1*M* and 1*A* (*A* = anorthic) ''polytypes'' (it should be noted that, strictly speaking, the compounds under consideration cannot be considered as polytypes, since they are not isochemical). It is of interest that rauchite is the only known example of the 1*A*-stacking type in the family of uranyl arsenate/phosphate decahydrates with medium-size divalent metal cations.

Acknowledgements: We are grateful to Stuart J. Mills and anonymous referee for their helpful comments and to Reto Gieré for the editorial work. Our studies were supported by the Russian Foundation for Basic Research (grants nos. 11-05-00397-a and 11-05-00407-a), grant of the internal budget of St. Petersburg State University (no. 3.37.84.2011) and the SPbSU X-ray Diffraction Resource Center.

References

Chernorukov, N.G., Suleimanov, E.V., Dzhabarova, S.T. (1998): Synthesis and study of compounds formed in the systems $Ni(PUO_6)_2$ – H_2O and $Ni(AsUO_6)_2$ – H_2O. *Z. Neorg. Khim.*, **43**, 997–1002 (in Russian).

Dymkov, Y.M., Kazantsev, V.V., Lyubchenko, V.A. (1970): Incrustate carbonate veins of the uranium-arsenide deposit. *in Uranium deposits: zonality and parageneses*. Atomizdat, Moscow, 205–244 (in Russian).

Granovskaya, N.V. (1984): Mineralogy and thermobarogeochemistry of the Belorechenskoye barite deposit (North-Western Caucaus). *Zapiski VMO.*, **113**, **4**, 454–463 (in Russian).

Krivovichev, V.G. (1972): *Dolomites and ankerites of the Belorechenskoye deposit and some aspects of investigation of magnesium-iron carbonates. Vestnik Leningradskogo Gosudarstvennogo Universiteta*, ser. 6. *Geology*, **1**, 36–44 (in Russian).

— (1973): Mineralogical-geochemical features and problems of genesis of the Belorechenskoye barite deposit. PhD thesis. Leningrad State University (in Russian).

— (1975): Physical-chemical conditions of formation of some low-temperature hydrothermal deposits (at the example of the Belorechenskoye deposit). *Zapiski VMO.*, **104**, **4**, 377–388 (in Russian).

Locock, A.J. (2007a): Crystal chemistry of actinide phosphates and arsenates. *in* ''*Structural chemistry of inorganic actinide compounds*'', S.V. Krivovichev, P.C. Burns, I.G. Tananaev, eds., chap. 6, Elsevier, Amsterdam, 217–278.

— (2007b): Trends in actinide compounds with the autunite sheet-anion topology. *Zapiski RMO.*, **136**, **7**, 115–137.

Locock, A.J., Burns, P.C., Flynn, T.M. (2004): Divalent transition metals and magnesium in structures that contain the autunite type sheet. *Can. Mineral.*, **42**, 1699–1718.

Melkov, V.G. & Sergeeva, A.M. (1971): Mineralogy of Dakhovskoye and Pskentskoye uranium deposits at Northern Caucasus. *in* ''*Materials on geology of uranium deposits: information collection*'', 15, VIMS, Moscow, 22–40 (in Russian).

Miller, S.A. & Taylor, J.C. (1986): The crystal structure of saleeite, $Mg(UO_2PO_4)_2 \cdot 10H_2O$. *Z. Kristallogr.*, **177**, 247–253.

Pekov, I.V. (1993): Minerals of the nickeline – breithauptite series from the Belorechenskoye deposit (Northern Caucasus). *Zapiski VMO.*, **122**, **3**, 44–49 (in Russian).

Pekov, I.V., Levitskiy, V.V., Krivovichev, V.G. (2010): Mineralogy of the Belorechenskoye deposit (Northern Caucasus, Russia). *Mineral. Almanac*, **15**, **2**, 1–91.

Pekov, I.V., Levitskiy, V.V., Krivovichev, S.V., Zolotarev Jr., A.A., Chukanov, N.V., Bryzgalov, I.A., Zadov, A.E. (2012): New nickel-uranium-arsenic mineral species from oxidation zone of the Belorechenskoye deposit, Northern Caucasus, Russia. II. Dymkovite, $Ni(UO_2)_2(As^{3+}O_3)_2 \cdot 7H_2O$, a seelite-related arsenite. *Eur. J. Mineral.*, **24**, 923–930.

Plášil, J., Sejkora, J., Čejka, J., Novák, M., Viñalis, J., Ondruš, P., Veselovský, F., Škácha, P., Jehlička, J., Goliáš, V., Hloušek, J. (2010): Metarauchite, $Ni(UO_2)_2(AsO_4)_2 \cdot 8H_2O$, from Jáchymov, Czech Republic, and Schneeberg, Germany: a new member of the autunite group. *Can. Mineral.*, **48**, 335–350.

Semashko, A.P. & Pakul'nis, G.V. (1971): Geological structure and formation of the Dakhovskoye deposit. *in* ''*Materials on geology of uranium deposits: information collection*'', 14. VIMS, Moscow, 63–83 (in Russian).

Sheldrick, G.M. (2008): A short history of *SHELX*. *Acta Crystallogr.*, **A64**, 112–122.

Zubov, A.I. & Kazantsev, V.V. (1970): Post-ore mineralization in carbonate-arsenide-pitchblende veins. *in* ''*Uranium deposits: zonality and parageneses*'', Atomizdat, Moscow, 244–273 (in Russian).

Received 12 January 2012
Modified version received 24 February 2012
Accepted 2 March 2012